

Synthesis and characterization of sodium polyaspartate-functionalized silica-coated magnetite nanoparticles: A heterogeneous, reusable and magnetically separable catalyst for the solvent-free synthesis of 2-amino-4*H*-chromene derivatives

Akbar Mobinikhaledi¹  | Hassan Moghanian² | Masoumeh Ghanbari¹

¹Department of Chemistry, Faculty of Science, Arak University, Arak 38156-8-8349, Iran

²Department of Chemistry, Dezful Branch, Islamic Azad University, Dezful, Iran

Correspondence

Akbar Mobinikhaledi, Department of Chemistry, Faculty of Science, Arak University, Arak 38156-8-8349, Iran.
Email: akbar_mobini@yahoo.com

An efficient and facile method was used for the synthesis of sodium polyaspartate-functionalized silica-coated magnetite nanoparticles. The structure of this nanoparticle was characterized by scanning electron microscopies, X-ray diffraction, energy-dispersive X-ray, Fourier transform infrared spectroscopies and vibrating sample magnetometry. Then, this compound was used as a reusable heterogeneous catalyst for green synthesis of 2-amino-4*H*-chromene derivatives via one-pot three-component reactions. This novel material showed great catalytic performance and the reactions which were carried out by this catalyst showed good to excellent yields. Besides, the catalyst could easily be separated from the reaction mixture by using an external magnetic field and it was stable enough to reuse several times without any significant reduction in the yield of reactions. Eco-friendliness, high purity of the desired products, short reaction time and easy workup procedure can be mentioned as the other advantages of this method.

KEYWORDS

2-amino- 4*H*-chromenes, green chemistry, magnetic nanoparticles, multicomponent reactions

1 | INTRODUCTION

One-pot multicomponent reactions are very useful tools for the synthesis of organic compounds because of their low costs, least waste production, simple approach, short times, and environmentally friendliness. For this reason, medicinal and organic chemists have widely applied these reactions to synthesize biologically active compounds.^[1] Among biologically active compounds, 2-amino- 4*H*-chromenes have attracted a lot of attention due to their wide range of medicinal properties, such as spasmolytic, diuretic, anticoagulant, anticancer and anti-anaphylactic activity.^[2–9]

Recently, catalysts like lipase,^[10] Et₃N,^[11] Zn(L-proline)₂,^[12] p-toluenesulfonic acid (p-TSA),^[13] iodine,^[14] Meglumine,^[15] Silica functionalized propyl sulfonic acid,^[16] and ionic liquids^[17,18] have been used for the synthesis of chromene derivatives. However, these methods have some disadvantages including long reaction times, harsh reaction conditions and toxic catalysts. In order to avoid these limitations, scientists have intensely focused on developing efficient, reusable catalysts which shorten the reaction times.^[1–3]

On the other hand, nanoparticles do not have any of disadvantages mentioned above and they can be useful heterogeneous catalysts for synthesis of 2-amino-4*H*-

chromenes because they have high surface areas. However, the application of these compounds as catalysts has been limited due to their tedious recovery procedures which resulted from their small sizes. Also, remarkable amounts of these solid catalysts are lost during the separation process. Therefore, scientists have used magnetic nanoparticles (MNPs), like Fe_3O_4 , as catalysts for the synthesis of biologically active compounds to solve this problem because not only they have high surface areas but also they can be easily separated by using an external magnetic field.^[19]

Besides, using magnetic nanoparticles as catalysts is associated with other advantages including easy synthesis and functionalization, low toxicity and low cost. However, magnetic nanoparticles can easily aggregate into larger clusters because of their anisotropic dipolar attraction. In addition, they have other deficiencies such as leaching under acidic conditions and being susceptible to autoxidation and toxicity. Therefore, it is necessary to protect the surface of MNPs in order to reduce these undesirable features. For this purpose, MNPs are usually coated with a polymeric or inorganic matrix.^[20] Among inorganic compounds, SiO_2 can be a suitable candidate for protecting the surface of MNPs due to its high chemical and thermal stability and most importantly its easy modification by a wide range of functional groups, which increase chemical and colloidal stability of these compounds.^[21–23]

The objective of the present work was to develop a more efficient synthetic process for the synthesis of 2-amino-4*H*-chromene derivatives (Scheme 1). Herein, sodium polyaspartate-functionalized silica-coated magnetite nanoparticles were prepared and its catalytic performance for synthesis of 2-amino-4*H*-chromenes was investigated. The method was very useful because of the considerable efficiency of the catalyst and its environmental compatibility. Also, the catalyst was inexpensive and highly efficient and it could easily be recovered and reused.

2 | RESULTS AND DISCUSSION

2.1 | Synthesis and structural characterization of MNPs-SPAsp as catalyst

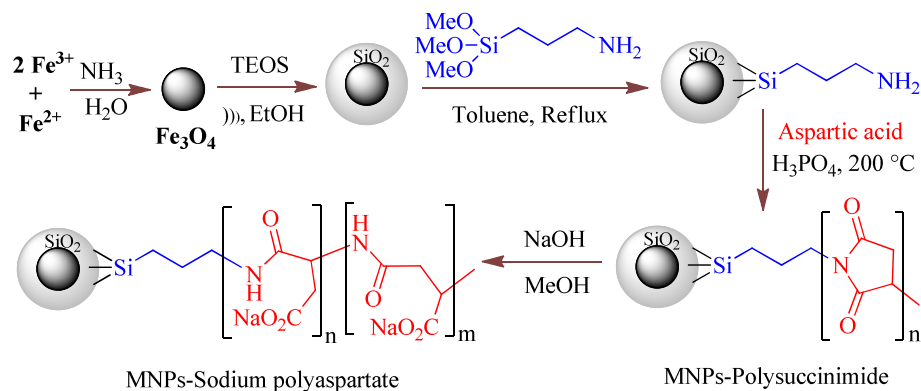
Magnetic nanoparticles (MNPs) are considered to be attractive as heterogeneous supports in catalytic



SCHEME 1 Multicomponent synthesis of 2-amino-4*H*-chromenes using sodium polyaspartate-functionalized silica-coated magnetite nanoparticles

transformation due to the high surface area, easy preparation and functionalization and facile removing with aid of external magnet from the reaction mixture. As shown in Scheme 2, the MNPs-SPAsp magnetic nanoparticle was synthesized in five steps from commercially available materials. Magnetite Fe_3O_4 nanoparticles were prepared by the simple co-precipitation of iron (II) and iron (III) ions in basic solution, according to the reported literature.^[22,24] Considering the aggregation tendency of the Fe_3O_4 nanoparticles and acid corrosion problem, the synthesized MNPs were coated by silica using a sol-gel process. The $\text{Fe}_3\text{O}_4@\text{SiO}_2$ core-shell structures were then sequentially treated with 3-aminopropyltrimethoxysilane (APTS) to obtain 3-aminopropyl magnetic nanoparticles ($\text{Fe}_3\text{O}_4@\text{SiO}_2\text{-NH}_2$) substrate. Next, poly(succinimide)-functionalized magnetic silica nanoparticles (MNPs-PSI) were obtained from thermal polymerization of pre-formed $\text{Fe}_3\text{O}_4@\text{SiO}_2\text{-NH}_2$ with *L*-aspartic acid using *o*-phosphoric acid as a dehydration agent. The amino groups in $\text{Fe}_3\text{O}_4@\text{SiO}_2\text{-NH}_2$ can act as nucleophilic groups and attack the carbonyl group of *L*-aspartic acid to build a stable and compact coating on the magnetic core. Finally, hydrolysis of surface MNPs-PSI nanoparticles with NaOH solution gives biodegradable sodium polyaspartate-functionalized magnetic silica nanoparticles (MNPs-SPAsp).

The structure of MNPs-SPAsp was characterized by Fourier transform infrared spectroscopy (FT-IR), scanning electron microscopy (SEM), energy dispersive spectrometry (EDS), X-ray powder diffraction (XRD), N_2 adsorption and desorption, vibrating sample magnetometry (VSM) and thermogravimetry (TG). Figure 1 shows the FT-IR spectra of Fe_3O_4 , $\text{Fe}_3\text{O}_4@\text{SiO}_2$, $\text{Fe}_3\text{O}_4@\text{SiO}_2\text{-NH}_2$, MNPs-PSI and MNPs-SPAsp nanoparticles. The characteristic absorption of Fe-O from magnetic nanoparticle cores was observed at about 579 cm^{-1} (Figure 1a). Compared with Fe_3O_4 , Figure 1b presented an intense adsorption peak at 1088 cm^{-1} and three weak peaks at 962 , 808 and 455 cm^{-1} , which could be ascribed to the asymmetric stretching, symmetric stretching, in plane bending and rocking mode of the Si-O-Si group respectively, in the SiO_2 shell. Moreover, the O-H stretching vibration modes (Si-OH) near 3400 cm^{-1} and H-O-H twisting vibration mode near 1620 cm^{-1} were observed for both (Figure 1a and Figure 1b). Figure 1c shows the FT-IR spectrum of $\text{Fe}_3\text{O}_4@\text{SiO}_2\text{-NH}_2$ nanoparticles. In comparison with $\text{Fe}_3\text{O}_4@\text{SiO}_2$ characteristic absorption bonds are the same, demonstrating the existence of SiO_2 components. In addition, the new bands are observed at 2949 and 2872 cm^{-1} (CH_2), indicating the definite graft of 3-aminopropyl group. According to FT-IR spectra of MNPs-PSI nanoparticles (Figure 1d), the symmetric stretching bond of imide group at 1722 cm^{-1} demonstrated that the poly(succinimide) (PSI) was successfully



SCHEME 2 Preparation of sodium polyaspartate-functionalized silica-coated nano-Fe₃O₄ particles

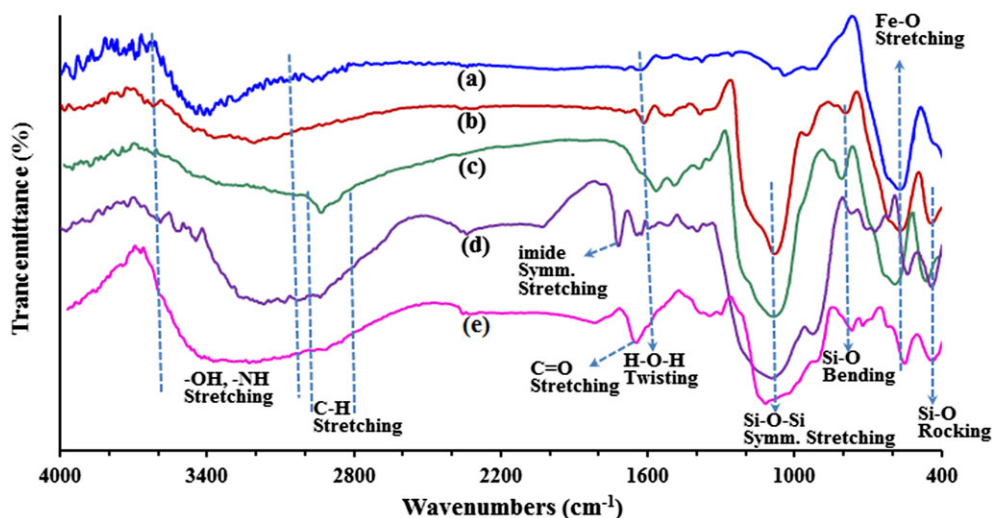


FIGURE 1 FT-IR spectra of (a) Fe₃O₄, (b) Fe₃O₄@SiO₂, (c) Fe₃O₄@SiO₂-NH₂, (d) MNPs-PSI and (e) MNPs-SPAsp

conjugated to the surface of the magnetic nanoparticles. The FT-IR of MNPs-SPAsp illustrates characteristic peaks at 1651 cm⁻¹ (C = O stretching), which is derived from hydrolysis of surface MNPs-PSI nanoparticles, clearly

indicating the formation of polyaspartate layers on magnetic nanoparticles.

Next, the morphology and nanoparticle size of the synthesized magnetic MNPs-SPAsp catalyst was characterized

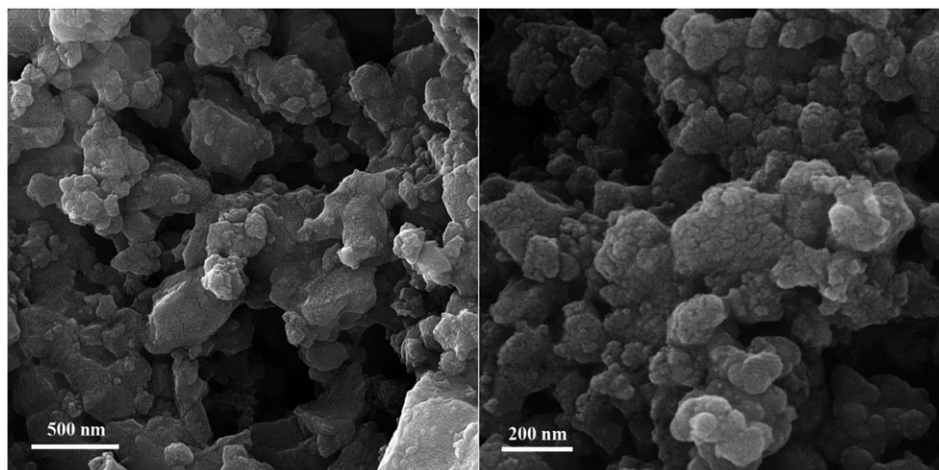


FIGURE 2 Low-magnification (right) and high-magnification (left) FE-SEM images of MNPs-SPAsp nanoparticles

by field emission scanning electron microscopy (FE-SEM) (Figure 2). As shown in Figure 2, the catalyst particles possess near spherical morphology with average diameter of about 30–50 nm. Furthermore, SEM images show some aggregation, which was illustrated the successful grafting of the polymer on to magnetic nanoparticles. The component of MNPs-SPAsp was analyzed by using an energy dispersive spectrometer (EDS) (Figure 3). Figure 3 confirms the presence of Na in the structure of the catalyst. Moreover, Si, O, and Fe signals can be seen in EDS analysis indicating that the iron oxide particles were loaded into silica. Also, the signal related to Si is more intense than those related to Fe showing that SiO_2 trapped the Fe_3O_4 nanoparticles.

The thermal stability of the MNPs-SPAsp catalyst was determined using TGA analysis and the results were shown in Figure 4. Two steps of decomposition were observed in TGA curve of the MNPs-SPAsp catalyst. In the first step, the weight loss of 6.30% below 140 °C was assigned to the removal of physically trapped solvents and surface hydroxyl groups. The second step involves the decomposition of 13.35% over the range of 140–550 °C which is due to the decomposition of the coating organic moiety in the nanocomposite. Based on this mass loss, it was calculated that 0.82 mmol of SPAsp was loaded on 1 g of the MNPs-SPAsp catalyst.

XRD measurements were used to investigate the presence as well as the degree of crystallinity of both magnetic Fe_3O_4 and the MNPs-SPAsp catalyst (Figure 5). Both of these compounds showed the same patterns, indicating that the crystalline spinel ferrite core remained intact during the silica-coating process. The XRD data of the synthesized magnetic nanoparticles appeared diffraction peaks at $2\theta = 30.4, 35.8, 43.3, 53.9, 57.3, 63.0,$ and 74.5 which can be assigned to the (220), (311), (400), (422), (511), (440) and (533) planes of Fe_3O_4 , respectively. This pattern proves that the Fe_3O_4 particles of the MNPs-SPAsp

nanoparticles were pure with a cubic spinel structure and they are perfectly matched with the standard Fe_3O_4 sample (JCPDS card no. 85–1436). The broad peak from $2\theta = 20$ to 27 (Figure 5B) is related to an amorphous silica phase in the shell of the silica-coated Fe_3O_4 nanoparticles ($\text{Fe}_3\text{O}_4@\text{SiO}_2$).^[17] The average crystallite size of the magnetic nanoparticles can be estimated by the (311) XRD peak and Scherrer's formula ($D = 0.9\lambda/\beta \cos \theta$). In this formula, D is defined as the average crystalline size, λ is the X-ray wave-length (0.154 nm), β is the full width in radians subtended by the half maximum intensity width of the (311) powder peak, and θ belongs to the Bragg angle of the (311) peak in degrees.^[18] According to the data, the crystallite size of the magnetic nanoparticle was obtained 13.3 nm by using Scherrer's equation. The crystallite size obtained by XRD was smaller than that obtained by FE-SEM analysis (Figure 2). This difference can be explained by the fact that crystallite sizes are considered as the sizes of 'coherently diffracting domains' of crystals in XRD measurements while grains may contain several types of these domains.

Also, the magnetic properties of the nanoparticles were studied by using the vibrating sample magnetometer (VSM). Figure 6 illustrates the magnetization curves of Fe_3O_4 and MNPs-SPAsp nanoparticles. The magnetization of samples was completely saturated at high fields of up to 8000.0 Oe and the M_s of MNPs-SPAsp nanoparticles decreased from 43.3 to 17.6 emu g^{-1} upon coating Fe_3O_4 core with silica and functionalizing with polyaspartate. Also, the hysteresis loops indicate the super-paramagnetic behavior of the Fe_3O_4 and MNPs-SPAsp particles in which the M_r and the H_c are close to zero ($M_r = 0.85$ and 0.49 emu g^{-1} , and $H_c = 4.9$ and 8.71 Oe , respectively).^[19] The strong magnetization of the nanoparticles was also proved by using an external magnet.

The surface characteristics of the MNPs-SPAsp nanoparticles were investigated by nitrogen adsorption at 77 K.

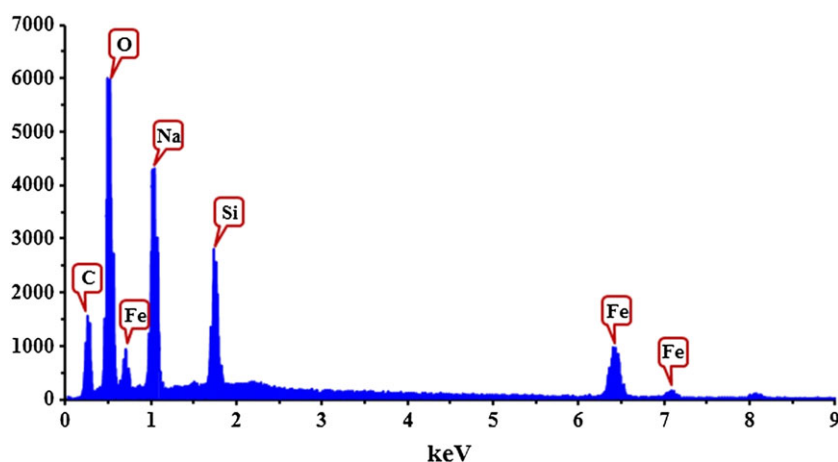


FIGURE 3 The EDS spectrum of MNPs-SPAsp nanoparticles

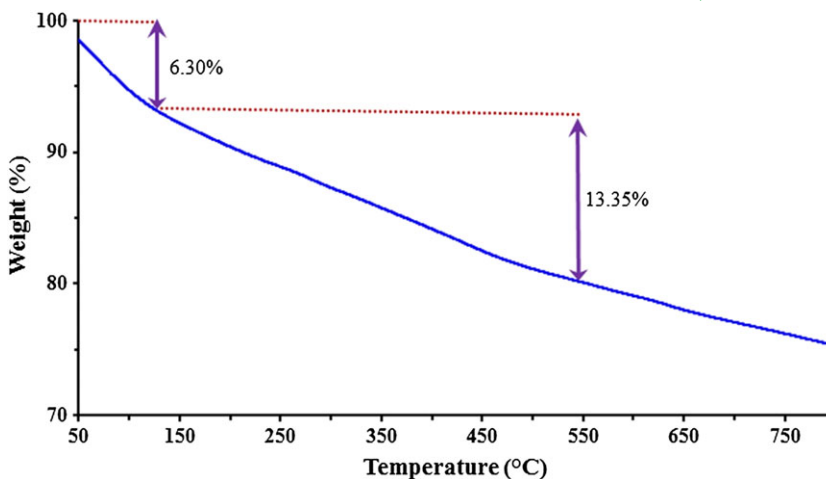


FIGURE 4 Thermal gravimetric analysis (TGA) of MNPs-SPAsp

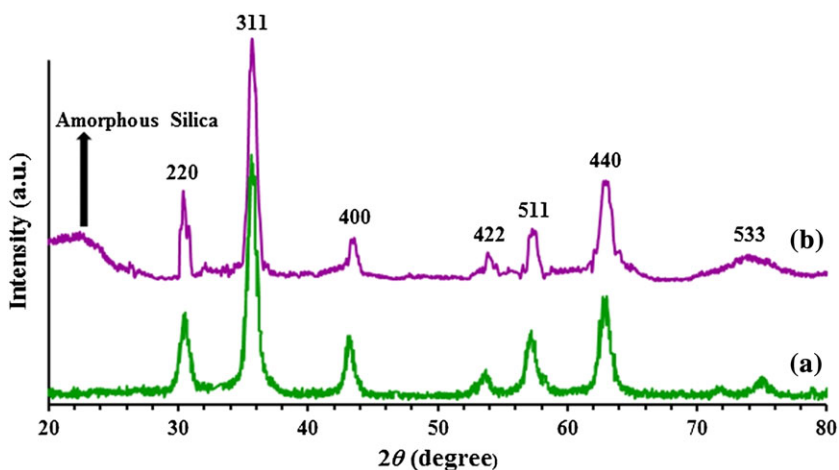


FIGURE 5 The XRD diffraction pattern of Fe_3O_4 (a) and MNPs-SPAsp (b)

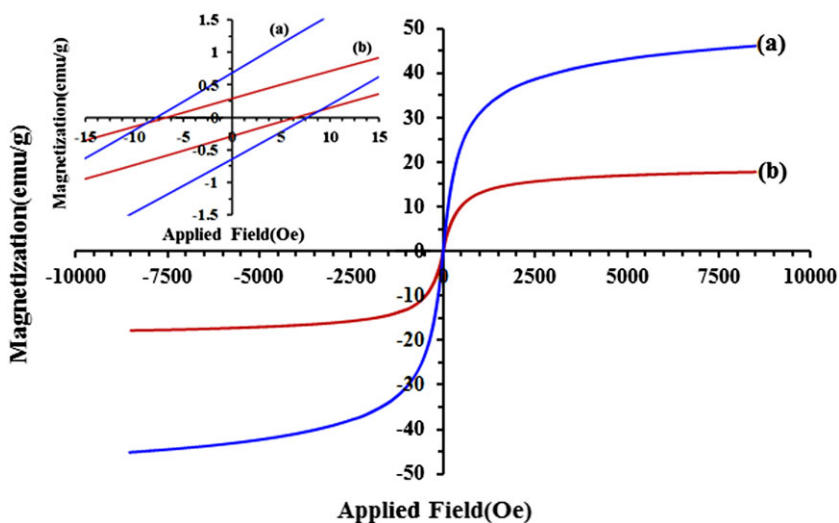


FIGURE 6 Magnetization curves for the prepared Fe_3O_4 MNPs (a) and MNPs-SPAsp nanoparticles at room temperature (b) left inset: The magnified field from -15 to 15 Oe

Figure 7 illustrates BJH plot and adsorption–desorption isotherm of the catalyst. This isotherm was type IV indicating mesoporous nature of the material. Furthermore,

the narrow hysteresis loop observed in the isotherm of the MNPs–SPAsp nanoparticles proves the porous nature of this material.^[20] According to results of these analyses,

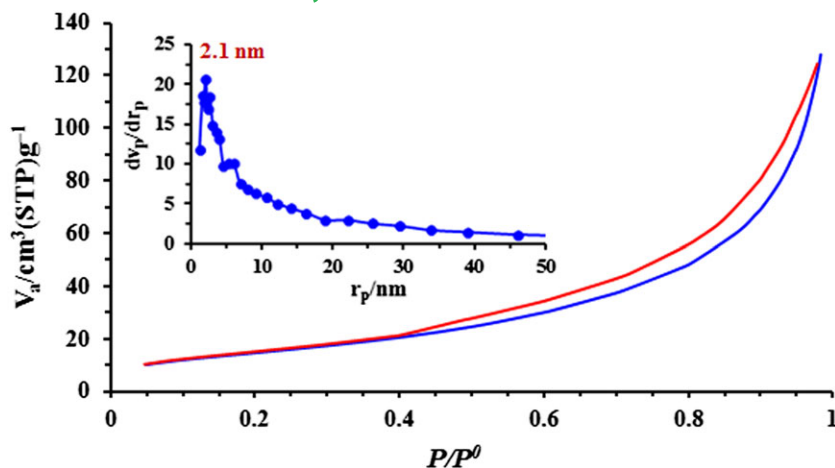


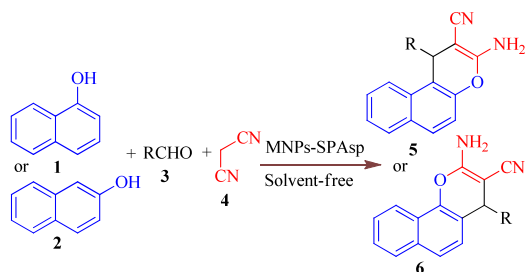
FIGURE 7 Nitrogen adsorption isotherms and BJH plot for MNPs-SPAsp nanoparticles

BET-surface area (S_{BET}) and total pore volume (V_p) were $55.11 \text{ m}^2 \text{ g}^{-1}$ and $0.199 \text{ cm}^3 \text{ g}^{-1}$, respectively. Moreover, the BJH plot showed an average pore diameter of 2.1 nm for this material.

2.2 | Catalytic studies

The catalytic performance of this novel basic organo-catalyst has been studied for the synthesis of 2-amino-4*H*-chromenes (Scheme 3 and Scheme 4). To find the optimized conditions, the reaction of 2-naphthol **1** (1 mmol), benzaldehyde **3** (1 mmol) and malononitrile **4** (1.2 mmol) was used as a model, and variables affecting on the reaction yields such as the type of solvent, the amount of catalyst, different temperatures, and solvent-free conditions were studied (Table 1). As shown in Table 1, conventional heating at 120 °C under solvent-free conditions is more efficient (Table 1, entry 7) over the organic solvents, because of its considerable efficiency and environmental compatibility.

In order to prove the generality and efficacy of the catalyst, malononitrile and different kinds of aldehyde, containing either electron-donating or electron-withdrawing groups, were reacted with one of these reagents: β -naphthol, α -naphthol, dimedone or ethyl acetate. The

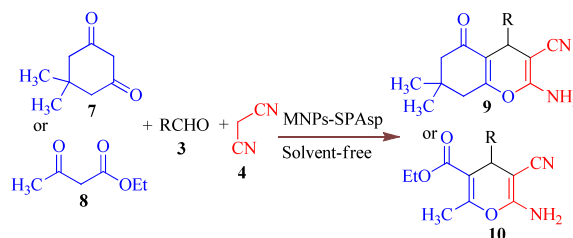


SCHEME 3 The one-pot three component reaction of aldehyde, malononitrile and α - or β -naphthol catalyzed by MNPs-SPAsp nanoparticles

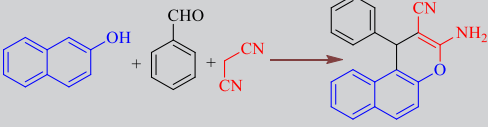
results were summarized in Tables 2 and 3. These reactions were very efficient and the desired products were obtained in good to excellent yields (85–97%) in relatively short reaction times, without formation of byproducts.

Also, since a wide range of inorganic or organic catalysts were used for the synthesis of 2-amino-4*H*-chromenes, we decided to gather the results obtained by these catalysts for the synthesis of both 3-amino-1-phenyl-1*H*-benzo[*f*]chromene-2-carbonitrile and 2-amino-7,7-dimethyl-5-oxo-4-phenyl-5,6,7,8-tetrahydro-4*H*-chromene-3-carbonitrile under optimized conditions in order to compare the catalytic performance of our catalyst with the reported inorganic or organic ones. Tables 4 and 5 compare catalytic performance of different catalysts in the synthesis of these two compounds. It can be concluded from these Tables that the MNPs-SPAsp catalyst can be considered as one of the best catalysts for these reaction because of their short reaction times, simple conditions and environmental friendliness. Most importantly, the advantages related to the inherent magnetic properties have distinguished the efficiency of this catalyst.

Scheme 5 illustrates the possible mechanism for the reactions catalyzed by MNPs-SPAsp. The formation of the products can be rationalized by initial Knoevenagel condensation reaction between an aldehyde and malononitrile anion; then, the first intermediate reacted



SCHEME 4 The one-pot three component reaction of aldehyde, malononitrile and dimedone or ethyl acetoacetate catalyzed by MNPs-SPAsp nanoparticles

TABLE 1 Optimization of reaction conditions for the synthesis of 2-amino-4-phenyl-4*H*-benzo[*f*]chromene-3-carbonitrile (Table 2, entry 1)^a


Entry	Catalyst (mg)	Solvent	Condition	Time (h)	Yield (%) ^b
1	MNPs-SPAsp(50)	EtOH	R.T.	24	<10
2	MNPs-SPAsp(50)	EtOH	Reflux	12	60
3	MNPs-SPAsp(50)	EtOH-H ₂ O (1:1)	Reflux	12	48
4	MNPs-SPAsp(50)	CH ₃ CN	Reflux	12	58
5	MNPs-SPAsp(50)	CHCl ₃	Reflux	12	56
6	MNPs-SPAsp(50)	Solvent-free	85 °C	2	38
7	MNPs-SPAsp(50)	Solvent-free	120 °C	0.5	93
8	MNPs-SPAsp(20)	Solvent-free	120 °C	1.5	62
9	MNPs-SPAsp(100)	Solvent-free	120 °C	0.5	93
10	-	Solvent-free	120 °C	4	Trace
11	Fe ₃ O ₄ (50)	Solvent-free	120 °C	3	30
12	Fe ₃ O ₄ @SiO ₂ (50)	Solvent-free	120 °C	3	28
13	MNPs-NH ₂ (50)	Solvent-free	120 °C	3	65
14	MNPs-PSI (50)	Solvent-free	120 °C	3	20

^aBenzaldehyde (1 mmol), 2-naphthol (1 mmol), malononitrile(1.2 mmol).^bIsolated yields.

with the compounds containing hydroxyl group (β -naphthol, α -naphthol, dimedone or ethyl acetate) through Michael addition reaction to produce the second

intermediate. Then, an intramolecular cyclization followed by the elimination of H⁺ gives the final products.

TABLE 2 MNPs-SPAsp mediated synthesis of 2-amino-4*H*-chromene derivatives with aldehydes, malononitrile and β -naphthol or α -naphthol

Entry	Ar	Naphthol	Product	Time (min)	Yield (%) ^a	M.P. (°C)	
						Found	Reported ^{Lit.}
1	C ₆ H ₅	β -naphthol	5a	30	93	295–296	297–299 ^[25]
2	4-NO ₂ C ₆ H ₄	β -naphthol	5b	25	96	188–189	187–189 ^[26]
3	4-FC ₆ H ₄	β -naphthol	5c	40	87	234–236	233–234 ^[27]
4	4-MeC ₆ H ₄	β -naphthol	5d	45	91	253–254	255–256 ^[15]
5	4-MeOC ₆ H ₄	β -naphthol	5e	50	90	187–188	185–187 ^[28]
6	2-ClC ₆ H ₄	β -naphthol	5f	30	85	255–256	257–259 ^[29]
7	4-N(me) ₂ C ₆ H ₄	β -naphthol	5 g	60	89	226–228	225–228 ^[30]
8	4-OH-3-MeOC ₆ H ₃	β -naphthol	5 h	50	86	250–251	252–253 ^[31]
9	4-(iso-Pr) C ₆ H ₄	β -naphthol	5i	75	85	209–211	-
10	C ₆ H ₅	α -naphthol	6j	30	95	211–212	213–215 ^[26]
11	4-OHC ₆ H ₄	α -naphthol	6 k	15	96	188–190	190–192 ^[26]
12	4-BrC ₆ H ₄	α -naphthol	6 l	45	92	235–237	239–241 ^[32]
13	4-ClC ₆ H ₄	α -naphthol	6 m	30	89	241–243	245–246 ^[15]
14	3-NO ₂ C ₆ H ₄	α -naphthol	6n	15	97	210–212	214–215 ^[33]

^aIsolated yields.

TABLE 3 MNPs-SPAsp mediated synthesis of 2-amino-4*H*-chromene derivatives with aldehydes, malononitrile and dimedone or ethyl acetoacetate

Entry	Ar	β -Dicarbonyl	Product	Time (min)	Yield (%) ^a	M.P. (°C)	
						Found	Reported ^{Lit.}
1	C ₆ H ₅	Dimedone	9o	30	92	227–228	228–230 ^[34]
2	4-BrC ₆ H ₄	Dimedone	9p	25	97	197–199	196–198 ^[35]
3	2-ClC ₆ H ₄	Dimedone	9q	30	88	198–200	201–205 ^[36]
4	4-OH-3-MeOC ₆ H ₃	Dimedone	9r	45	86	228–229	230–232 ^[37]
5	Thiophene-2-carbaldehyde	Dimedone	9 s	30	82	193–195	191–194 ^[38]
6	3-Pyridyl	Dimedone	9 t	60	84	198–200	-
7	3-NO ₂ C ₆ H ₄	Ethyl acetoacetate	10u	60	75	172–173	174–176 ^[39]
8	4-ClC ₆ H ₄	Ethyl acetoacetate	10v	75	72	171–173	170–172 ^[40]
9	4-MeOC ₆ H ₄	Ethyl acetoacetate	10w	90	70	130–133	135 ^[41]

^aIsolated yields**TABLE 4** Comparison of MNPs-SPAsp with some reported catalysts for synthesis of 3-amino-1-phenyl-1*H*-benzo[*f*]chromene-2-carbonitrile^a

Entry	Catalyst (amount)	Condition	Time	Yield(%) ^b	Ref.
1	Nano-Bi ₂ WO ₆ (5 mol%)	H ₂ O, R.T.	20 min	86	[30]
2	Imidazole (0.2 mmol)	EtOH, reflux	1 h	86	[25]
3	TBAC (10 mol%) ^c	Solvent-free, 100 °C	35 min	82	[42]
4	Nano CP (0.01 g) ^d	H ₂ O, reflux	20 min	95	[29]
5	POPI (5 mol%) ^e	Ball milling, ambient	13 min	97	[26]
6	ZnFe ₂ O ₄ NPs (40 mg)	H ₂ O, R.T.	3 h	93	[43]
7	Saturated K ₂ CO ₃ (10 ml)	H ₂ O, mw	3.2 min	90	[44]
8	Gel entrapped DABCO (1 g)	EtOH, ambient	10 min	93	[45]
9	CAN (5 mol%)	Solvent-free, 120 °C	30 min	91	[46]
10	[bmim]OH (0.5 mmol)	H ₂ O, reflux	60 min	90	[33]
11	Na ₂ CO ₃ (0.1 mmol)	Solvent-free, 125 °C	40 min	100	[47]
12	SBA-DABCO (0.125 g)	H ₂ O, 80 °C	25 min	87	[48]
13	5-Å MS (0.5 g)	Solvent-free, MW	5 min	95	[49]
14	Fe ₃ O ₄ /SiO ₂ /propyl-pip (0.05 g)	Solvent-free, 120 °C	40 min	95	[50]
15	MNPs-SPAsp (50 mg)	Solvent-free, 120 °C	30 min	93	This work

^aReaction conditions: Benzaldehyde (1 mmol), β -naphthol (1 mmol), malononitrile (1.2 mmol).^bIsolated yields; ^ctetrabutylammonium chloride; ^dNanozeolite clinoptilolite; ^epotassium phthalimide

2.3 | Catalytic recyclability

Because the recovery and reusability of the catalyst are very important for commercial and industrial purposes as well as green process considerations, the recovery and reusability of MNPs-SPAsp was investigated in the sequential reaction of 3-nitrobenzaldehyde (1 mmol), α -naphthol (1 mmol), malononitrile (1.2 mmol) and the catalyst (0.05 g) under solvent-free conditions at 120 °C. The results were shown in Table 6. The catalyst could be reused at least six times without any significant loss in the yield of reactions. The stability of the recovered

catalysts was confirmed by FT-IR spectroscopy (Figure 8). The FT-IR spectrum of the recycled catalyst after six runs was very identical to that of fresh catalyst, confirming that the catalyst indicates excellent performance for the synthesis of 2-amino-4*H*-chromenes.

3 | EXPERIMENTAL

3.1 | General

All reagents were used without further purification and were procured from commercial sources. Melting points

TABLE 5 Comparison of MNPs-SPAsp with some reported catalysts for synthesis of 2-amino-7,7-dimethyl-5-oxo-4-phenyl-5,6,7,8-tetrahydro-4*H*-chromene-3-carbonitrile^a

Entry	Catalyst (amount)	Condition	Time	Yield(%) ^b	Ref.
1	Ni(NO ₃) ₂ ·6H ₂ O (10 mol%)	H ₂ O, reflux	20 min	95	[51]
2	Urea (10 mol%)	EtOH-H ₂ O (1:1), R.T.	3 h	90	[39]
3	MSNs (10 mg) ^c	EtOH, 60 °C	15 min	94	[36]
4	Meglumine (5 mol%)	EtOH-H ₂ O, (1:1), R.T.	5 min	97	[15]
5	POPINO (5 mol %) ^d	H ₂ O, reflux	15 min	95	[52]
6	Fe ₃ O ₄ @SiO ₂ /DABCO (0.05 g)	H ₂ O, 80 °C	25 min	90	[53]
7	γ-Fe ₂ O ₃ @hap-Si-(CH ₂) ₃ -AMP (1.5 mol%)	H ₂ O, reflux	10 min	80	[38]
8	TBAB (10 mol%) ^e	H ₂ O, reflux	40 min	90	[54]
9	SBPPSP (0.05 g) ^f	EtOH-H ₂ O, (1:1), reflux	25 min	90	[40]
10	Nano-NH ₄ H ₂ PO ₄ /Al ₂ O ₃ (0.03 g)	EtOH, reflux	15 min	86	[34]
11	[cmmim]Br (10 mol%)	Solvent-free, 110 °C	5 min	90	[37]
12	Na ₂ CO ₃ (10 mol%)	Ball milling, R.T.	25 min	99	[35]
13	Nano CP (0.01 g) ^g	H ₂ O, reflux	15 min	95	[55]
14	MNPs-SPAsp (50 mg)	Solvent-free, 120 °C	30 min	92	This work

^aReaction conditions: Benzaldehyde (1 mmol), dimedone (1 mmol), malononitrile (1.2 mmol).

^bIsolated yields;

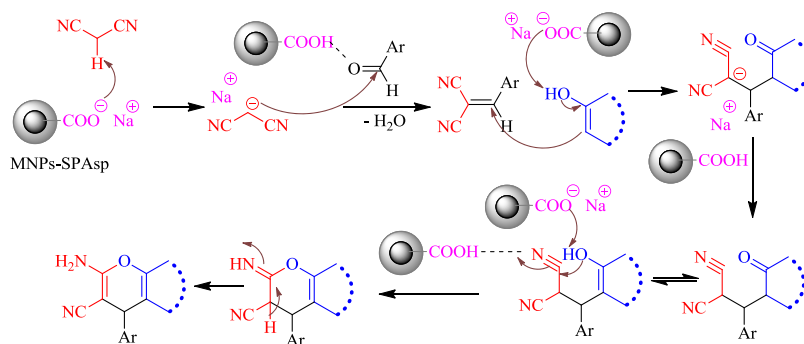
^cMesoporous Silica Nanoparticles;

^dPotassium phthalimide-N-oxyl;

^eTetrabutylammonium Bromide;

^fSilica-bonded N-propylpiperazine sodium n-propionate;

^gNanozeolite clinoptilolite



SCHEME 5 The possible mechanism for one-pot synthesis of 2-amino-4*H*-chromenes using MNPs-SPAsp nanoparticles

were determined on Electrothermal 9200 apparatus. Elemental analysis was performed on a Vario EL III elemental analyzer. Analytical thin layer chromatography (TLC) was performed using Merck 0.2 mm silica gel 60 F-254 Al-plates. The FTIR spectrum of the sample was recorded on a Unicam Galaxy Series FT-IR 5000 spectrophotometer at region of 4000–400 cm⁻¹ using pressed KBr discs. The ¹H and ¹³C NMR spectra were recorded on a Bruker Avance spectrometer operating at 400 and 100 MHz for ¹H and ¹³carbon, respectively in DMSO-*d*₆ with TMS as an internal standard. The X-ray diffraction (XRD) was performed on Philips X-Pert (Cu-Kα radiation,

λ = 0.15405 nm) in the range of 2θ = 20–80° using 0.04° as the step length. The specific surface area and the pore size distribution were calculated by the Brunauer–Emmett–Teller (BET) method and Barrett–Joyner–Halenda (BJH) model, respectively. The particle size and external morphology of the particles were carried out on a Hitachi S-4700 field emission-scanning electron microscope (FE-SEM). The magnetization and hysteresis loop were measured at room temperature using a Vibrating Sample Magnetometer (Model 7300 VSM system, Lake Shore Cryotronic, Inc., Westerville, OH, USA). The thermogravimetric analysis (TGA) and differential thermal

TABLE 6 Recyclability of MNPs-SPAsp in reaction of 3-nitrobenzaldehyde (1 mmol), α -naphthol (1 mmol), malononitrile (1.2 mmol) and catalyst (0.05 g) under solvent-free conditions^a

Run	Yield(%)
1	97
2	95
3	95
4	94
5	93
6	91

^aTime of reaction was 15 min.

gravimetric (DTG) data for MNPs-SPAsp were done using a Mettler TA4000 System. About 10 mg of samples was heated from room temperature to 800 °C with a heating rate of 10 °C min⁻¹ in nitrogen atmosphere.

3.2 | Preparation of the magnetic Fe₃O₄ nanoparticles (MNPs)

Fe₃O₄ nanoparticles are prepared by chemical coprecipitation of Fe³⁺ and Fe²⁺ described in the literature.^[22,24] Briefly, FeCl₂·4H₂O (0.9941 g, 5 mmol) and FeCl₃·6H₂O (2.7029 g, 10 mmol) were dissolved in 100 ml of deionized water in a three-necked round bottomed flask (250 mL). The resulting solution is heated for 1 h at 80 °C under N₂ atmosphere. Consequently, 10 mL of concentrated ammonia (25%) were added quickly. After 1 h, the mixture was cooled to room temperature and magnetic nanoparticles were isolated by magnetic decantation, first washed with distilled water, then ethanol, and finally dried under vacuum at room temperature.

3.3 | Synthesis of silica-coated MNPs (Fe₃O₄@SiO₂ MNPs)

The Fe₃O₄@SiO₂ core-shell nanoparticles were prepared according to the Stober method.^[56] Typically, 500 mg of the synthesized magnetite nanoparticles were dispersed by ultrasonic vibration in a mixture of ethanol (20 ml), deionized water (3 ml) and 1 ml of 25 wt% concentrated aqueous ammonia solution for 20 min. Subsequently, 0.7 ml of tetraethylorthosilicate (TEOS) was added dropwise. After stirring for 12 h at room temperature under N₂ atmosphere, the products were collected from the solution using a magnet, and then washed several times with water and ethanol and dried at 25 °C under vacuum.

3.4 | Synthesis of 3-aminopropyl-functionalized magnetic silica nanoparticles (Fe₃O₄@SiO₂-NH₂ MNPs)

500 mg Fe₃O₄@SiO₂ nanoparticles were dispersed into 50 ml toluene and sonicated for 20 min, followed by the addition of 0.5 mL (3-aminopropyl) trimethoxysilane (APTES). Then, the mixture was refluxed at 110 °C with continuous stirring for 12 h under a nitrogen flow. The resulting functionalized Fe₃O₄@SiO₂ was collected by magnetic separation followed by washing with toluene and ethanol several times and drying at 60 °C for 6 h.

3.5 | Synthesis of poly(succinimide)-functionalized magnetic silica nanoparticles (MNPs-PSI)

The MNPs-PSI magnetic nanoparticles were prepared according to the procedure described in the literature.^[57] for synthesis of poly(succinimide) with some modifications as follows: 500 mg of MNPs-PSI is dispersed in 85%

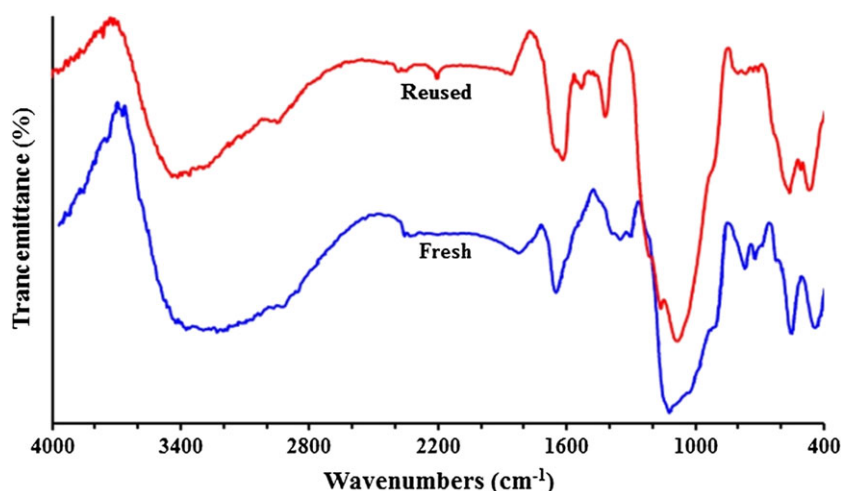


FIGURE 8 FT-IR spectra of the fresh catalyst and the six-times reused catalyst

o-phosphoric acid (2 g) in an ultrasonic bath for 20 min, followed by the addition of L-aspartic acid (ASP) (1.5 g, 11.3 mmol). The reaction mixture was then stirred for 8 h, under nitrogen atmosphere at 200 °C. The product was dispersed several times in water by ultrasonic vibration and collected by magnetic separation until it was neutral. It was subsequently washed with hot DMSO and with methanol and then was dried at 85 °C under vacuum to yield MNPs-PSI.

3.6 | Synthesis of sodium polyaspartate-functionalized magnetic silica nanoparticles (MNPs-SPAsp)

The hydrolysis of MNPs-PSI was carried out as follows: 500 mg of MNPs-PSI nanoparticles were added to 10 ml of NaOH 5% solution and then ultrasonically dispersed for 20 min. After stirring for 1 h at room temperature under N₂ atmosphere, the resulting product was collected by magnetic separation followed by washing with water and ethanol several times and drying at 40 °C for 6 h under reduced pressure.

3.7 | Acid–base titrations of MNPs-SPAsp

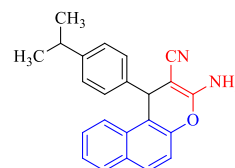
The concentration of carboxyl groups was quantitatively estimated by back titration using NaOH (0.01 N). 5 ml of 0.01 M HCl solution was added to 0.05 g of the magnetic nanoparticles and the mixture was stirred for 30 min. The catalysts were magnetically separated and washed with deionized water. The sample was back-titrated with the 0.01 M NaOH solution in the presence of phenolphthalein as indicator. Averages of three separate titrations were performed to obtain an average value for the concentration of dissociable COOH groups. The acid–base titration results revealed 0.02 mmol/g carboxyl groups amount.

3.8 | General procedure for the synthesis of 2-amino-4H-chromene derivatives

To a mixture of aromatic aldehyde (1 mmol), malonitrile (1.2 mmol), and enolizable C-H activated compound (1 mmol), MNPs-SPAsp (0.05 g) was added as a catalyst, and the mixture was magnetically stirred under thermal solvent-free condition on a preheated oil bath at 120 °C for the appropriate time. After completion of the reaction as indicated by TLC (using *n*-hexane-ethylacetate as eluent), the resulting mixture was diluted with hot ethanol (10 ml) and the catalyst separated by an external magnet and washed with hot distilled water (5 ml) and ethanol (3 ml) two times. The filtrate was cooled down to room

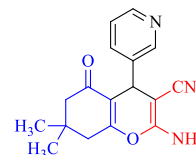
temperature and the crude products which precipitated were collected and recrystallized from ethanol if necessary.

3.9 | Characterization data for new compounds



Compound 5i (Table 2, Entry 9):

IR (KBr): ν_{\max} = 3427, 3335, 3209, 2958, 2191, 1649, 1411, 1234, 1082, 1037, 812, 750 cm⁻¹; ¹H NMR (400 MHz, DMSO-*d*₆): δ = 7.89–7.98 (m, 2H), 7.87 (d, *J* = 7.2 Hz, 1H), 7.40–7.49 (m, 2H), 7.34 (d, *J* = 8.8 Hz, 1H), 7.15–7.06 (m, 4H), 6.96 (br, 2H), 5.26 (s, 1H), 2.84–2.74 (m, 1H), 1.13 (d, *J* = 5.2 Hz, 6H). ¹³C NMR (100 MHz, DMSO-*d*₆): δ = 159.7, 146.7, 146.5, 143.1, 130.8, 130.1, 129.3, 128.4, 127.1, 126.8, 126.6, 124.9, 123.6, 120.6, 116.8, 115.9, 58.0, 37.6, 32.9, 23.7. Analytical calculation for C₂₃H₂₀N₂O: C, 81.15; H, 5.92; N, 8.23. Found: C, 81.22; H, 5.95, N, 8.19.



Compound 9t (Table 3, Entry 6):

IR (KBr): ν_{\max} = 3394, 3323, 3211, 2958, 2204, 1660, 1425, 1369, 1249, 1215, 1140, 1028, 711, 628, 561, 489 cm⁻¹; ¹H NMR (400 MHz, DMSO-*d*₆): δ = 8.42–8.37 (m, 2H), 7.55 (d, *J* = 8.0 Hz, 1H), 7.36–7.30 (m, 1H), 7.13 (br, 2H), 4.26 (s, 1H), 2.54 (d, *J* = 5.2 Hz, 2H), 2.26 and 2.12 (AB system, *J* = 16.0 Hz, 2H), 1.04 (s, 3H), 0.96 (s, 3H). ¹³C NMR (100 MHz, DMSO-*d*₆): δ = 195.7, 162.9, 158.6, 148.6, 147.8, 140.0, 134.7, 123.6, 199.5, 111.8, 57.3, 49.9, 39.6, 33.4, 31.8, 28.2, 26.9. Analytical calculation for C₁₇H₁₇N₃O₂: C, 69.14; H, 5.80; N, 14.23. Found: C, 69.20; H, 5.86, N, 14.17.

4 | CONCLUSIONS

In conclusion, the synthesis of polyaspartate-functionalized silica-coated magnetite nanoparticles was performed by using a very simple, efficient and inexpensive method. The structure of this nanoparticle was characterized by using the following techniques: FT-IR, XRD, TG/DTG, FE-ESM, EDS, VSM and acid–base titration. Then, synthesis of 2-amino-4H-chromenes was carried out by using

a facile, versatile, one-pot multicomponent reaction and the new synthesized material was used as an efficient, magnetically separable and reusable heterogeneous catalyst for these reactions. This method has some advantages over the previous methods. High catalytic activity, generality, high yields, short reaction times, simple experimental procedure and easy work-up procedure are among these advantages.

ORCID

Akbar Mobinikhaledi  <http://orcid.org/0000-0002-9732-7282>

REFERENCES

- [1] J. Safaei-Ghomi, N. Enayat-Mehri, F. Eshteghal, J. Saudi Chem. Soc. **2017**, <https://doi.org/10.1016/j.jscs.2017.1005.1007>.
- [2] A. Kakanejadifard, F. Azarban, N. Khosravani, B. Notash, *J. Mol. Liq.* **2016**, *221*, 211.
- [3] S. Pradhan, V. Sahu, B. G. Mishra, *J. Mol. Catal. A: Chem.* **2016**, *425*, 297.
- [4] M. N. Elinson, A. N. Vereshchagin, S. I. Bobrovsky, R. F. Nasybullin, A. I. Ilovaisky, V. M. Merkulova, *C. R. Chim.* **2016**, *19*, 293.
- [5] S. Zavar, *Arab. J. Chem.* **2017**, *10*, S67.
- [6] B. Wu, X. Gao, Z. Yan, M.-W. Chen, Y.-G. Zhou, *Org. Lett.* **2015**, *17*, 6134.
- [7] G.-D. Yin, T.-T. Lai, Z.-S. Yan, H. Chen, J. Zheng, Q. Tao, *Tetrahedron* **2013**, *69*, 2430.
- [8] G. Yin, H. Shi, L. Xu, X. Wei, Q. Tao, *Synthesis* **2013**, *45*, 334.
- [9] A. F. Mahmoud, A. El-Latif, F. Fathy, A. M. Ahmed, *Chin. J. Chem.* **2010**, *28*, 91.
- [10] F. Yang, H. Wang, L. Jiang, H. Yue, H. Zhang, Z. Wang, L. Wang, *RSC Adv.* **2015**, *5*, 5213.
- [11] A. Shaabani, R. Ghadari, S. Ghasemi, M. Pedarpour, A. H. Rezayan, A. Sarvary, S. W. Ng, *J. Comb. Chem.* **2009**, *11*, 956.
- [12] B. Maleki, S. Babaee, R. Tayebee, *Appl. Organomet. Chem.* **2015**, *29*, 408.
- [13] R. Ghahremanzadeh, T. Amanpour, A. Bazgir, *J. Heterocycl. Chem.* **2009**, *46*, 1266.
- [14] G. Yin, L. Fan, T. Ren, C. Zheng, Q. Tao, A. Wu, N. She, *Org. Biomol. Chem.* **2012**, *10*, 8877.
- [15] R.-Y. Guo, Z.-M. An, L.-P. Mo, R.-Z. Wang, H.-X. Liu, S.-X. Wang, Z.-H. Zhang, *ACS Comb. Sci.* **2013**, *15*, 557.
- [16] P. Gholamzadeh, G. M. Ziarani, N. Lashgari, A. Badiei, P. Asadiatouei, *J. Mol. Catal. A: Chem.* **2014**, *391*, 208.
- [17] H. R. Shaterian, M. Mohammadnia, *J. Mol. Liq.* **2013**, *177*, 353.
- [18] P. Sharma, M. Gupta, R. Kant, V. K. Gupta, *RSC Adv.* **2016**, *6*, 32052.
- [19] W. Injumba, P. Ritprajak, N. Insin, *J. Magn. Magn. Mater.* **2017**, *427*, 60.
- [20] S. H. Araghi, M. H. Entezari, *Appl. Surf. Sci.* **2015**, *333*, 68.
- [21] M. A. Bodaghifard, A. Mobinikhaledi, S. Asadbegi, *Appl. Organomet. Chem.* **2017**, <https://doi.org/10.1002/aoc.3557>.
- [22] H. Moghanian, A. Mobinikhaledi, A. G. Blackman, E. Sarough-Farahani, *RSC Adv.* **2014**, *4*, 28176.
- [23] M. B. Gawande, P. S. Branco, R. S. Varma, *Chem. Soc. Rev.* **2013**, *42*, 3371.
- [24] K. Can, M. Ozmen, M. Ersoz, *Colloids Surf., B* **2009**, *71*, 154.
- [25] M. Nasim Khan, S. Pal, S. Karamthulla, L. H. Choudhury, *RSC Adv.* **2014**, *4*, 3732.
- [26] M. G. Dekamin, M. Eslami, *Green Chem.* **2014**, *16*, 4914.
- [27] J. Albadi, A. Mansournezhad, M. Darvishi-Paduk, *Chin. Chem. Lett.* **2013**, *24*, 208.
- [28] M. Farahi, B. Karami, S. Alipour, L. Taghavi Moghadam, *Acta Chim. Slov.* **2014**, *61*, 94.
- [29] S. M. Baghbanian, N. Rezaei, H. Tashakkorian, *Green Chem.* **2013**, *15*, 3446.
- [30] B. Paplall, S. Nagaraju, P. Veerabhadraiah, P. Sujatha, S. Kanvah, B. V. Kumar, D. Kashinath, *RSC Adv.* **2014**, *4*, 54168.
- [31] A. R. Moosavi-Zare, M. A. Zolfigol, O. Khaledian, V. Khakyzadeh, M. Darestani Farahani, M. H. Beyzavi, H. G. Kruger, *Chem. Eng. J.* **2014**, *248*, 122.
- [32] J. M. Khurana, B. Nand, P. Saluja, *Tetrahedron* **2010**, *66*, 5637.
- [33] K. Gong, H.-L. Wang, D. Fang, Z.-L. Liu, *Catal. Commun.* **2008**, *9*, 650.
- [34] B. Maleki, S. Sedigh Ashrafi, *RSC Adv.* **2014**, *4*, 42873.
- [35] O. Hosseinchi Qareaghaj, S. Mashkouri, M. R. Naimi-Jamal, G. Kaupp, *RSC Adv.* **2014**, *4*, 48191.
- [36] Y. Sarrafi, E. Mehrasbi, A. Vahid, M. Tajbakhsh, *Chin. J. Catal.* **2012**, *33*, 1486.
- [37] A. R. Moosavi-Zare, M. A. Zolfigol, O. Khaledian, V. Khakyzadeh, M. Darestani Farahani, H. G. Kruger, *New J. Chem.* **2014**, *38*, 2342.
- [38] M. Khoobi, M. Ma'mani, F. Rezazadeh, Z. Zareie, A. R. Foroumadi, A. Ramazani, A. Shafiee, *J. Mol. Catal. A: Chem.* **2012**, *359*, 74.
- [39] G. Brahmachari, B. Banerjee, *ACS Sustainable Chem. Eng.* **2014**, *2*, 411.
- [40] K. Niknam, N. Borazjani, R. Rashidian, A. Jamali, *Chin. J. Catal.* **2013**, *34*, 2245.
- [41] A. Molla, E. Hossain, S. Hussain, *RSC Adv.* **2013**, *3*, 21517.
- [42] H. Mehrabi, N. Kamali, *J. Iran Chem. Soc.* **2012**, *9*, 599.
- [43] P. Das, A. Dutta, A. Bhaumik, C. Mukhopadhyay, *Green Chem.* **2014**, *16*, 1426.
- [44] M. Kidwai, S. Saxena, M. K. Rahman Khan, S. S. Thukral, *Bioorg. Med. Chem. Lett.* **2005**, *15*, 4295.
- [45] S. Shinde, G. Rashinkar, R. Salunkhe, *J. Mol. Liq.* **2013**, *178*, 122.
- [46] A. Kumar, S. Sharma, R. A. Maurya, J. Sarkar, *J. Comb. Chem.* **2010**, *12*, 20.
- [47] M. R. Naimi-Jamal, S. Mashkouri, A. Sharifi, *Mol. Diversity* **2010**, *14*, 473.
- [48] J. Davarpanah, A. R. Kiasat, *RSC Adv.* **2014**, *4*, 4403.

- [49] A. C. Shekhar, A. R. Kumar, G. Sathaiah, K. Raju, P. S. Rao, M. Sridhar, P. V. Banda Narsaiah, S. S. Srinivas, B. Sridhar, *Helv. Chim. Acta.* **2012**, *95*, 502.
- [50] A. Mobinikhaledi, H. Moghanian, Z. Souri, *Lett. Org. Chem.* **2014**, *11*, 432.
- [51] B. Boumoud, A. A. Yahiaoui, T. Boumoud, A. Debache, *J. Chem. Pharm. Res.* **2012**, *4*, 795.
- [52] M. G. Dekamin, M. Eslami, A. Maleki, *Tetrahedron* **2013**, *69*, 1074.
- [53] J. Davarpanah, A. R. Kiasat, S. Noorzadeh, M. Ghahremani, *J. Mol. Catal. A: Chem.* **2013**, *376*, 78.
- [54] A. Mobinikhaledil, M. A. Bodaghi Fard, *Acta Chim. Slov.* **2010**, *57*, 931.
- [55] S. M. Baghbanian, N. Rezaei, H. Tashakkorian, *Green Chem.* **2010**, *12*, 1481.
- [56] W. Stöber, A. Fink, E. J. Bohn, *J. Colloid Interface Sci.* **1968**, *26*, 62.
- [57] T. Nakato, A. Kusuno, T. Kakuchi, *J. Polym. Sci. Pol. Chem.* **2000**, *38*, 117.

How to cite this article: Mobinikhaledi A, Moghanian H, Ghanbari M. Synthesis and characterization of sodium polyaspartate-functionalized silica-coated magnetite nanoparticles: A heterogeneous, reusable and magnetically separable catalyst for the solvent-free synthesis of 2-amino-4*H*-chromene derivatives. *Appl Organometal Chem.* 2017;e4108. <https://doi.org/10.1002/aoc.4108>